Polyhedron 67 (2014) 513–519

Contents lists available at ScienceDirect

Polyhedron

journal homepage: www.elsevier.com/locate/poly

Syntheses, crystal structures and copper-binding capabilities of amidate-hanging platinum mononuclear complexes containing alkylamine moieties

Kazuhiro Uemura *, Yuko Sugiyama, Erina Yasuda, Masahiro Ebihara

Department of Chemistry and Biomolecular Science, Faculty of Engineering, Gifu University, Yanagido 1-1, Gifu 501-1193, Japan

ARTICLE INFO

Article history:
Received 1 August 2013
Accepted 19 September 2013
Available online 14 October 2013

Keywords:
Platinum
Crystal structure
Alkyl
Hydrophobic
Multinuclear complex

ABSTRACT

As analogs of *cis*-$[Pt(piam)_2(NH_3)_2]\cdot 2H_2O$ (**1**, piam = pivalamidate), two kinds of platinum mononuclear complexes, *cis*-$[Pt(piam)_2(NH_2C_3H_7)_2]\cdot H_2O$ (**2**) and *cis*-$[Pt(piam)_2(NH_2C_4H_9)_2]$ (**3**), have been synthesized and characterized by single-crystal X-ray analyses. The square-planar complexes **2** and **3** contain propyl and butyl moieties, respectively, enhancing the hydrophobicity. Both compounds have non-coordinated oxygen atoms in the piam ligands that can bind to a second metal, such as the Cu^{2+} ion, to afford trinuclear Pt–Cu–Pt complexes. UV–Vis and electron paramagnetic resonance spectra of the reaction of **2** and **3** with the Cu^{2+} ion show that both compounds form dinuclear Pt–Cu complexes as intermediates.

1. Introduction

Extensive recent research into the design and synthesis of multinuclear complexes has provided a wide variety of structures [1–20]. Among them, heterometallic cluster complexes with metal–metal bonds are of particular importance because the cooperative redox on the metals plays an essential role in unique electron transfers and characteristic magnetisms [6–20]. For rational synthesis of Pt heterometal linear complexes, "amidate-hanging" Pt mononuclear complexes are suitable starting materials, because they can readily bind to a second metal ion with the non-coordinated oxygen atoms of the amidate moieties [16,21,22]. The mononuclear amidate complexes are prepared by utilizing direct base hydrolysis of the corresponding nitrile complexes [6,23–28]. Although these "amidate-hanging" Pt mononuclear complexes are potential modules for obtaining multinuclear linear complexes, only a few examples have been reported [22,29]. In this paper, we report the syntheses and crystal structures of two novel compounds containing relatively long alkyl amines (Scheme 1), *cis*-$[Pt(piam)_2(NH_2C_3H_7)_2]\cdot H_2O$ (**2**, piam = pivalamidate) and *cis*-$[Pt(piam)_2(NH_2C_4H_9)_2]$ (**3**), showing the second metal's binding capability.

2. Experimental

2.1. Materials

Potassium tetrachloroplatinate(II) was obtained from Tanaka Kikinzoku Co. $NH_2C_4H_9$, $NaClO_4$, $CuCl_2\cdot 2H_2O$ and KI were obtained from Nacalai Tesque Co. Pivalonitrile and $NH_2C_3H_7$ were obtained from Tokyo Chemical Industry Co. $AgNO_3$ was obtained from Wako Co. *Cis*-$[PtI_2(NH_2C_3H_7)_2]$ and *cis*-$[PtI_2(NH_2C_4H_9)_2]$ were synthesized by a modification of Dhara's method [30,31].

2.2. Synthesis of cis-$[Pt(piam)_2(NH_2C_3H_7)_2]\cdot H_2O$ (2)

An aqueous solution (4 mL) of K_2PtCl_4 (0.42 g, 1.0 mmol) was stirred with KI (0.68 g, 4.1 mmol) for 15 min at 40 °C, and then $NH_2C_3H_7$ (0.38 mL, 4.6 mmol) was added. After stirring for 1 day, a yellow powder of *cis*-$[PtI_2(NH_2C_3H_7)_2]$ was obtained. An aqueous solution (10 mL) of the yellow powder was stirred with $AgNO_3$ (0.34 g, 2.0 mmol) overnight in the dark, and AgI was then removed by filtration. The colorless filtrate was stirred with pivalonitrile (0.44 mL, 4.1 mmol) for 2 h, and then stirred for 1 day after addition of $NaClO_4$ (0.5 g, 4.1 mmol). The resulting white powder (0.41 g) was recrystallized from the mixed solution of Me_2CO (5 mL) and 1.0 M NaOH aqueous solution (10 mL) to obtain white crystals (0.19 g, 0.36 mmol) of *cis*-$[Pt(piam)_2(NH_2C_3H_7)_2]\cdot H_2O$. Yield 36%. Elemental analysis calcd for $C_{16}H_{40}N_4O_3Pt$: C, 36.15; H, 7.58; N, 10.54, found: C, 36.35; H, 7.18; N, 10.54%.

* Corresponding author. Tel./fax: +81 58 293 2561.
E-mail address: k_uemura@gifu-u.ac.jp (K. Uemura).

0277-5387/$ - see front matter © 2013 Elsevier Ltd. All rights reserved.
http://dx.doi.org/10.1016/j.poly.2013.09.037

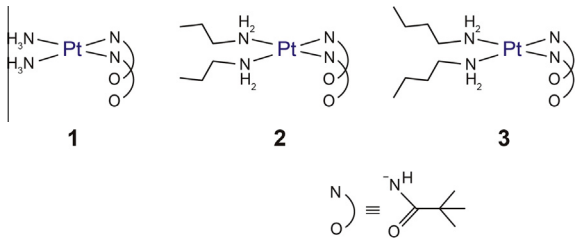

Scheme 1. Three kinds of amidate-hanging Pt mononuclear complex.

2.3. Synthesis of cis-[Pt(piam)$_2$(NH$_2$C$_4$H$_9$)$_2$] (**3**)

An aqueous solution (4 mL) of K_2PtCl_4 (0.42 g, 1.0 mmol) was stirred with KI (0.68 g, 4.1 mmol) for 15 min at 40 °C, and then $NH_2C_4H_9$ (0.45 mL, 4.5 mmol) was added. After stirring for 1 day, a yellow powder was obtained. An aqueous solution (10 mL) of the yellow powder was stirred with $AgNO_3$ (0.34 g, 2.0 mmol) overnight in the dark, and AgI was then removed by filtration. The colorless filtrate was stirred with pivalonitrile (0.44 mL, 4.1 mmol) for 4 h, and then stirred for 4 h after addition of $NaClO_4$ (0.5 g, 4.1 mmol). The resulting white powder (0.30 g) was recrystallized from the mixed solution of MeCN (1.5 mL) and 1.0 M NaOH aqueous solution (3 mL) to obtain a white powder. The white powder was recrystallized again from a mixed solution of Me_2CO (7 mL) and H_2O (7 mL) to obtain *cis*-[Pt(piam)$_2$(NH$_2$C$_4$H$_9$)$_2$] (85 mg, 0.16 mmol). Yield 16%. Elemental analysis calcd for $C_{18}H_{42}N_4O_2Pt$: C, 39.92; H, 7.82; N, 10.34, found: C, 39.29; H, 7.83; N, 10.17%.

2.4. Synthesis of [Pt$_2$Cu(piam)$_4$(NH$_2$C$_4$H$_9$)$_4$](PF$_6$)$_2$ (**4**)

A MeOH solution (8 mL) of $CuCl_2{\cdot}2H_2O$ (6.8 mg, 0.04 mmol) and **3** (65 mg, 0.12 mmol) was stirred for several minutes and mixed with an aqueous solution (0.5 mL) of $NaPF_6$ (25 mg, 0.15 mmol) at room temperature. After several days, light green crystals of [Pt$_2$Cu(piam)$_4$(NH$_2$C$_4$H$_9$)$_4$](PF$_6$)$_2$ were collected by filtration, washed with water and dried in vacuo (25 mg, 17 μmol). Yield 44%. Elemental analysis calcd for $C_{36}H_{84}CuF_{12}N_8O_4P_2Pt_2$: C, 30.10; H, 5.89; N, 7.80, found: C, 30.38; H, 6.01; N, 7.92%.

2.5. X-ray structure determination

Single crystals of **2**, **3** and **4** were mounted on a glass fiber and coated with epoxy resin. For each compound, X-ray data collection was carried out on a Rigaku AFC7R Mercury CCD diffractometer with graphite monochromated Mo Kα (λ = 0.71070 Å) radiation, operated at 15 kW power (50 kV, 300 mA). A total of 744 frames were collected using a scan width of 0.5° with an exposure time of 5 s/frame. Empirical absorption corrections [32] were performed for all data. The structures were solved by the direct method [33] with subsequent difference Fourier syntheses and refinement with SHELX-97 [34], operated by the YADOKARI-XG software package [35]. The crystal data and the details of the structure determination are summarized in Table 1. The non-hydrogen atoms were refined anisotropically and hydrogen atoms, except for the ones in the water molecule, were treated as riding atoms. Selected bond lengths and angles are shown in Table 2.

2.6. Physical measurements

The IR spectra were recorded on a Perkin Elmer Spectrum 400 over the range 400–4000 cm^{-1} at room temperature. UV–Vis spectra were recorded on a Shimadzu UV-3100PC over the range 340–1400 nm at room temperature. EPR spectra were measured on a JEOL TE-200 spectrometer. The field sweep was monitored with an Echo Electronics EFM-2000 ^{1}H NMR gaussmeter, the probe of which was attached beside the EPR cavity.

3. Results and discussion

3.1. Synthetic procedure

Taking advantage of a similar base-hydrolysis method as for *cis*-[Pt(piam)$_2$(NH$_3$)$_2$]·2H$_2$O (**1**) [22], we tried to obtain the desired compounds. However, it was not successful because their precursors, *cis*-[Pt(NC^{t}Bu)$_2$(NH$_2$C$_3$H$_7$)$_2$](ClO$_4$)$_2$ and *cis*-[Pt(NC^{t}Bu)$_2$(NH$_2$C$_4$H$_9$)$_2$](ClO$_4$)$_2$, do not dissolve in H_2O. This insolubility in H_2O is attributed to the hydrophobic alkyl chains on the amine moieties. For both compounds, the addition of organic solvents (Me_2CO or MeCN) accelerated the base hydrolysis to afford *cis*-[Pt(piam)$_2$(NH$_2$C$_3$H$_7$)$_2$]·H$_2$O (**2**) and *cis*-[Pt(piam)$_2$(NH$_2$C$_4$H$_9$)$_2$] (**3**), where the C≡N stretching bands in the IR spectra, 2306 and 2234 cm^{-1} for *cis*-[Pt(NC^{t}Bu)$_2$(NH$_2$C$_3$H$_7$)$_2$](ClO$_4$)$_2$, 2303 and 2234 cm^{-1} for *cis*-[Pt(NC^{t}Bu)$_2$(NH$_2$C$_4$H$_9$)$_2$](ClO$_4$)$_2$, disappeared (Fig. 1). In addition, the intense bands for the ClO_4^- ions in the IR spectra also disappeared, indicating that the positive charges of Pt^{2+} are compensated with negative charges on the piam ligands. As mentioned below, both **2** and **3** reacted with the Cu^{2+} ion to afford trinuclear Pt–Cu–Pt complexes in MeOH. However, only crystals of [Pt$_2$Cu(piam)$_4$(NH$_2$C$_4$H$_9$)$_4$](PF$_6$)$_2$ (**4**) were obtained by the addition of an aqueous $NaPF_6$ solution to the MeOH solution.

3.2. Crystal structure of cis-[Pt(piam)$_2$(NH$_2$C$_3$H$_7$)$_2$]·H$_2$O (**2**)

Fig. 2 shows the crystal structure of **2**. The square-planar coordination geometry around the Pt atom consists of two *cis* N atoms of propylamine and two *cis* N atoms of the piam ligands. The sum of the four *cis* N–Pt–N angles is 360.1°, which is indicative of their coplanarity. The C(1)=O(1) (1.271(5) Å) and C(6)=O(2) (1.260(5) Å) bond lengths are in agreement with double-bond character. On the other hand, the C(1)–N(3) (1.291(5) Å) and C(6)–N(4) (1.307(5) Å) bond distances are shorter than the usual C–N single bond distance, indicating a partial double-bond character. The bond distances and angles are essentially the same as those reported for **1** [22]. The crystal contains water molecules, which are hydrogen bonded to the oxygen atoms in the piam ligands with distances of 2.828(7) and 2.876(6) Å (Fig. 2b). An interesting feature of the crystal packing is that two complex molecules stack in a face-to-face fashion with eight hydrogen bonds between the amine moieties and oxygen atoms in the piam ligands, where the Pt–Pt distance is relatively short (3.4913(6) Å). The propyl moieties have different conformations with N(1)–C(11)–C(12)–C(13) and N(2)–C(14)–C(15)–C(16) torsion angles of 179.87(6) and 67.86(9)°, respectively.

3.3. Crystal structure of cis-[Pt(piam)$_2$(NH$_2$C$_4$H$_9$)$_2$] (**3**)

Fig. 3 shows the crystal structure of **3**. Compound **3** also has a square-planar coordination geometry around the Pt atom, consisting of two *cis* N atoms of butylamine and two *cis* N atoms of the piam ligands. The bond lengths in the amidate moieties are similar to those in **2**; C(1)=O(1) = 1.237(5) Å, C(6)=O(2) = 1.245(5) Å, C(1)–N(3) = 1.318(5) Å and C(6)–N(4) = 1.319(5) Å, which indicate double-bond character between the C and O atoms. Compound **3** crystallizes without solvent molecules. The butylamines groups hydrogen bond to oxygen atoms in the piam ligands on either side of the complex, resulting in a one-dimensional alignment (Fig. 3b).

Table 1
Crystallographic data and structure refinements for *cis*-$[Pt(piam)_2(NH_2C_3H_7)_2]\cdot H_2O$ (**2**), *cis*-$[Pt(piam)_2(NH_2C_4H_9)_2]$ (**3**) and $[Pt_2Cu(piam)_4(NH_2C_4H_9)_4](PF_6)_2$ (**4**).

	2	3	4
Empirical formula	$C_{16}H_{40}N_4O_3Pt$	$C_{18}H_{42}N_4O_2Pt$	$C_{36}H_{84}CuF_{12}N_8O_4P_2Pt_2$
Formula weight	531.61	541.65	1436.77
Crystal system	Monoclinic	Triclinic	Monoclinic
Space group	$P2_1/c$	$P\bar{1}$	$P2_1/n$
a (Å)	9.663(2)	10.336(4)	12.142(2)
b (Å)	14.939(4)	11.061(4)	17.369(3)
c (Å)	15.910(4)	11.292(4)	13.784(2)
α (°)	90	90.117(4)	90
β (°)	102.415 (3)	105.515(5)	98.030(2)
γ (°)	90	104.045(5)	90
V (Å^3)	2242.9 (9)	1203.8(7)	2878.6(8)
Z	4	2	2
Temperature (K)	293	293	293
Dc (Mg m^{-3})	1.574	1.494	1.658
Absorption coefficient (mm^{-1})	6.275	5.844	5.348
F (000)	1064	544	1422
Crystal size (mm^3)	0.23 × 0.21 × 0.19	0.30 × 0.20 × 0.10	0.40 × 0.40 × 0.30
Measured reflections	17703	9398	22844
Independent reflections	5133 [R_{int} = 0.0281]	5332 [R_{int} = 0.0196]	6594 [R_{int} = 0.0273]
Goodness-of-fit on F^2	1.062	1.073	1.144
R [$I > 2\sigma(I)$]	R_1 = 0.0313, wR_2 = 0.0665	R_1 = 0.0307, wR_2 = 0.0745	R_1 = 0.0410, wR_2 = 0.1074
R (all data)	R_1 = 0.0373, wR_2 = 0.0706	R_1 = 0.0349, wR_2 = 0.0772	R_1 = 0.0499, wR_2 = 0.1152

Table 2
Selected bond lengths (Å) and angles (°) for complexes **2**, **3** and **4**.

Complex 2			
Pt(1)–N(1)	2.062 (3)	Pt(1)–N(2)	2.073 (3)
Pt(1)–N(3)	2.003 (4)	Pt(1)–N(4)	2.018 (4)
C(1)–O(1)	1.271 (5)	C(6)–O(2)	1.260 (5)
C(1)–N(3)	1.291 (5)	C(6)–N(4)	1.307 (5)
N(1)–Pt(1)–N(2)	89.83 (13)	N(2)–Pt(1)–N(3)	92.02 (13)
N(3)–Pt(1)–N(4)	89.56 (13)	N(4)–Pt(1)–N(1)	88.65 (14)
Complex 3			
Pt(1)–N(1)	2.054 (3)	Pt(1)–N(2)	2.052 (4)
Pt(1)–N(3)	2.015 (3)	Pt(1)–N(4)	2.006 (4)
C(1)–O(1)	1.237 (5)	C(6)–O(2)	1.245 (5)
C(1)–N(3)	1.318 (5)	C(6)–N(4)	1.319 (5)
N(1)–Pt(1)–N(2)	90.51 (14)	N(2)–Pt(1)–N(3)	90.65 (15)
N(3)–Pt(1)–N(4)	87.59 (15)	N(4)–Pt(1)–N(1)	91.37 (14)
Complex 4			
Pt(1)–N(1)	2.065 (5)	Pt(1)–N(2)	2.072 (5)
Pt(1)–N(3)	2.000 (6)	Pt(1)–N(4)	1.999 (4)
C(1)–O(1)	1.265 (6)	C(6)–O(2)	1.274 (6)
C(1)–N(3)	1.310 (7)	C(6)–N(4)	1.293 (7)
Cu(1)–O(1)	1.963 (4)	Cu(1)–O(2)	1.966 (3)
Pt(1)–Cu(1)	2.6691 (4)	Pt(1)–Cu(1)–Pt(1*)	180
N(1)–Pt(1)–N(2)	90.4 (2)	N(2)–Pt(1)–N(3)	90.1 (2)
N(3)–Pt(1)–N(4)	87.8 (2)	N(4)–Pt(1)–N(1)	91.5 (2)
O(1)–Cu(1)–O(2)	90.74 (18)	O(1)–Cu(1)–O(1*)	180

Symmetry code.
* $-x+1, -y, -z+1$.

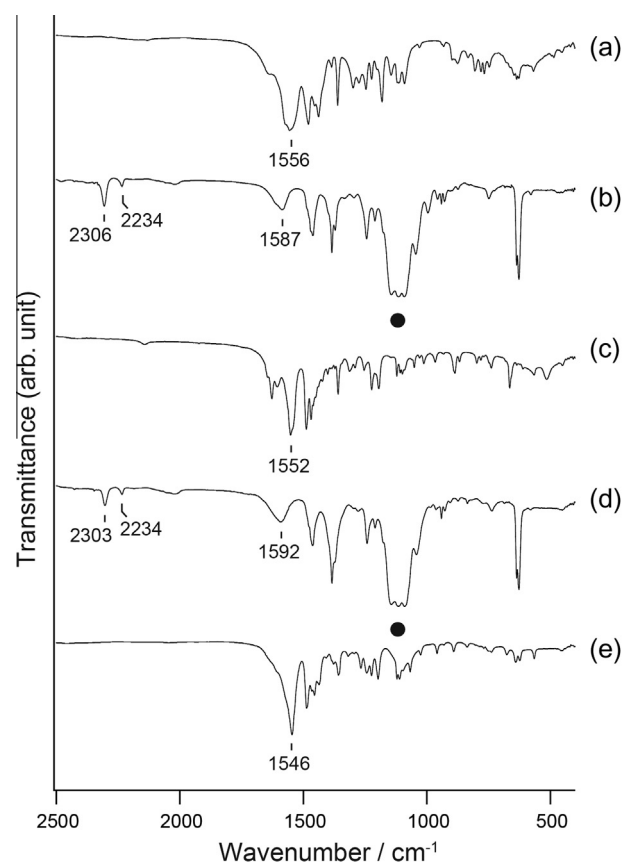

Fig. 1. IR spectra (KBr pellet) of (a) *cis*-$[Pt(piam)_2(NH_3)_2]\cdot 2H_2O$ (**1**), (b) *cis*-$[Pt(NC^tBu)_2(NH_2C_3H_7)_2](ClO_4)_2$, (c) *cis*-$[Pt(piam)_2(NH_2C_3H_7)_2]\cdot H_2O$ (**2**), (d) *cis*-$[Pt(NC^tBu)_2(NH_2C_4H_9)_2](ClO_4)_2$ and (e) *cis*-$[Pt(piam)_2(NH_2C_4H_9)_2]$ (**3**) at room temperature. Intense bands marked with filled circles are attributed to the ClO_4^- ions.

3.4. Crystal structure of $[Pt_2Cu(piam)_4(NH_2C_4H_9)_4](PF_6)_2$ (4)

By simply mixing **3** with $CuCl_2\cdot 2H_2O$ and $NaPF_6$ in $MeOH/H_2O$, the free oxygen atoms of the "amidate-hanging" Pt complex bind to Cu^{2+} ions to afford the heterometallic trinuclear complex $[Pt_2Cu(piam)_4(NH_2C_4H_9)_4](PF_6)_2$ (**4**). Fig. 4 shows the structure of the trinuclear complex in **4**. The Cu atom, located at an inversion center, is sandwiched by two Pt complexes through the four bridging piam ligands, affording a linear Pt–Cu–Pt alignment. The Pt–Cu distance is 2.6691(4) Å, which is similar to those in other Pt–Cu–Pt complexes [21,36–43]. However, it is slightly shorter than that in its ammonia analog $[Pt_2Cu(piam)_4(NH_3)_4](PF_6)_2$ (2.6870(6) Å) [20]. This shorter distance is attributed to the intramolecular hydrogen bonds between the N atoms of butylamine and the O atoms of the piam ligands; N–O = 2.962(6) and 3.031(6) Å. The dihedral angle between the Pt(1) and Cu(1) coordination planes is 15.1°, which is also smaller than that in $[Pt_2Cu(piam)_4(NH_3)_4]$

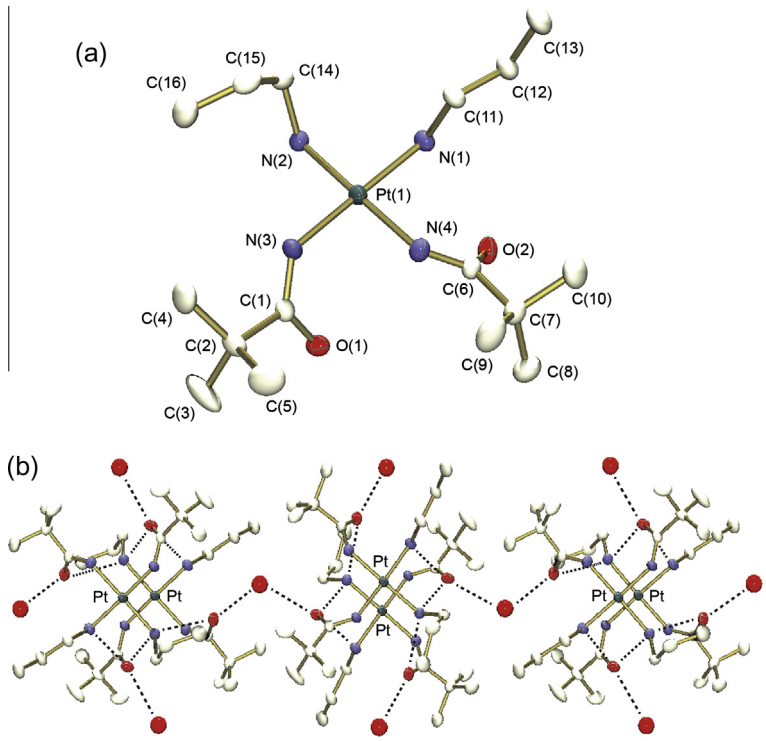

Fig. 2. (a) Structure of *cis*-[Pt(piam)$_2$(NH$_2$C$_3$H$_7$)$_2$]. (b) Packing view of *cis*-[Pt(piam)$_2$(NH$_2$C$_3$H$_7$)$_2$]·H$_2$O (**2**). Dotted lines indicate hydrogen bonds. The hydrogen atoms are omitted for clarity.

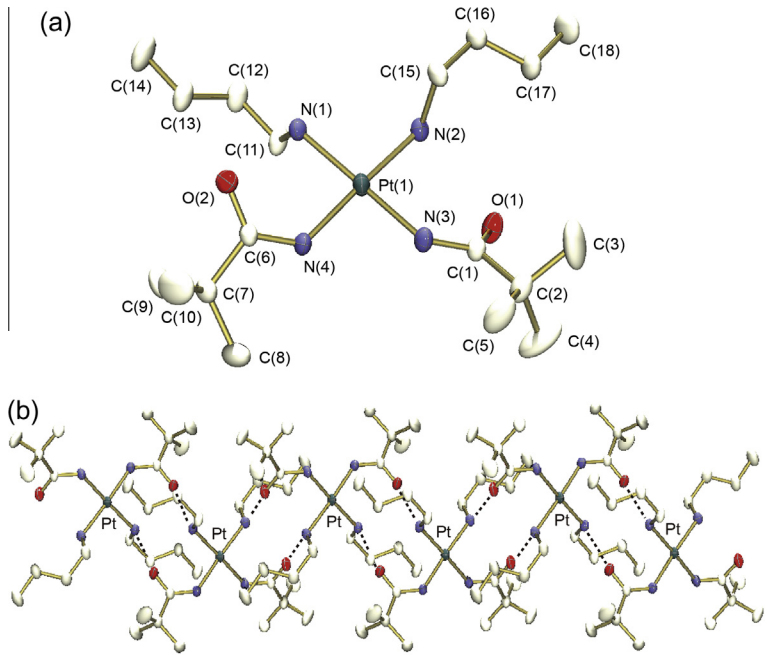

Fig. 3. (a) Structure of *cis*-[Pt(piam)$_2$(NH$_2$C$_4$H$_9$)$_2$] (**3**). (b) Packing view of **3**. Dotted lines indicate hydrogen bonds. The hydrogen atoms are omitted for clarity.

(PF$_6$)$_2$ (16.6°). The butyl moieties are directed perpendicular to the Pt coordination plane. Taking into account that the sum of the metal oxidation numbers in [Pt–Cu–Pt] is +6, the oxidation state of **4** is [Pt^{2+}–Cu^{2+}–Pt^{2+}]. Both the amine and amidate moieties hydrogen bond to PF_6^- ions with distances of 3.063(9)–3.337(15) Å, where every PF_6^- ion bridges two trinuclear units.

3.5. UV–Vis and EPR spectral titration of Cu^{2+} with **1**

Fig. 5a shows the UV–Vis spectra of CuCl$_2$·2H$_2$O (5 mM) in MeOH, with the addition of 0–3 equiv of **1**. As **1** is added, the absorption band around 870 nm, attributed to the *d–d* transition of the Cu^{2+} ion, decreases in intensity and a new absorption band

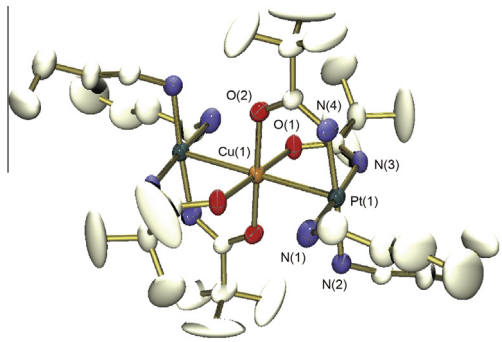

Fig. 4. Structure of $[Pt_2Cu(piam)_4(NH_2C_4H_9)_4]^{2+}$ in **4**. The hydrogen atoms are omitted for clarity.

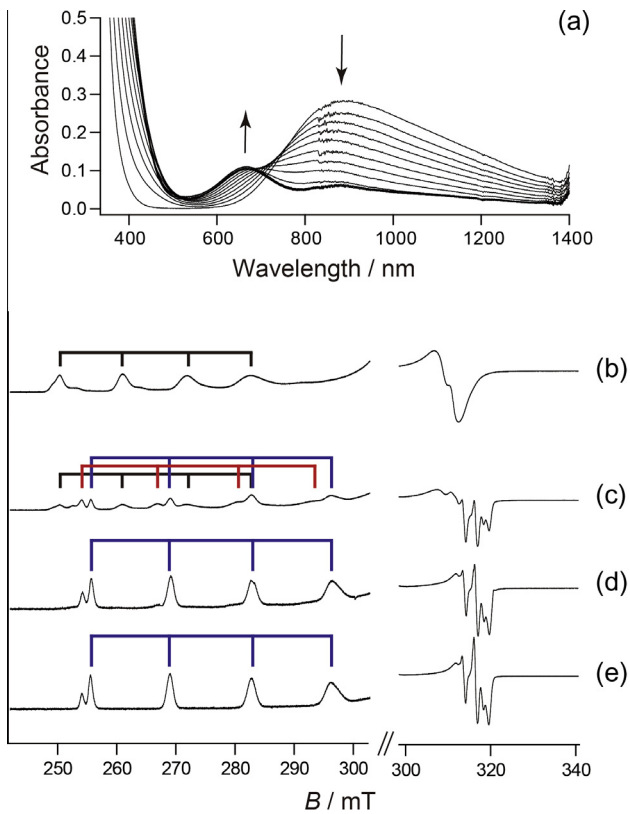

Fig. 5. (a) UV–Vis spectra of a 5 mM solution of $CuCl_2{\cdot}2H_2O$ in MeOH containing 0–3 equiv. of **1** at room temperature. Continuous wave EPR spectra in MeOH glass at 77 K for (b) $CuCl_2{\cdot}2H_2O$ (5 mM), mixture of $CuCl_2{\cdot}2H_2O$ (5 mM) and (c) **1** (5 mM), (d) **1** (10 mM), (e) **1** (15 mM). Experimental settings: microwave frequency, (b) 9.05751 GHz, (c) 9.05778 GHz, (d) 9.05887 GHz and (e) 9.05529 GHz; microwave power, 3 mW; field modulation, 0.2 mT.

around 660 nm appears, indicating that the Cu^{2+} ion interacts with **1** [20,44]. The decrease of the absorption band around 870 nm was terminated when 2 equiv of **1** was added, showing that this reaction affords a 1:2 adduct [20].

Fig. 5b shows the electron paramagnetic resonance (EPR) (X-band) spectrum of $CuCl_2{\cdot}2H_2O$ in MeOH glass at 77 K. The spectrum shows a well-resolved profile with $g_{//} = 2.429$ and $g_{\perp} = 2.096$, which is characteristic of the unpaired electron residing in the Cu dx^2–y^2 orbital [45–48]. The $g_{//}$ signal is split into four components by the hyperfine interaction ($A_{//} = 122 \times 10^{-4}\ cm^{-1}$) with the Cu nucleus ($I = 3/2$). Another smaller signal with $g_{//} = 2.377$, $g_{\perp} = 2.083$, and $A_{//} = 139 \times 10^{-4}\ cm^{-1}$ was also observed, which may be attributed to the different coordination environments caused by Cl^- ions.

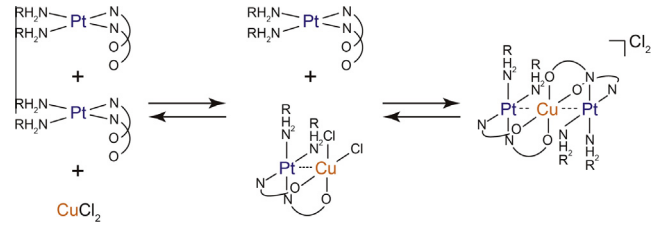

Scheme 2. Reaction of $CuCl_2$ and amidate-hanging Pt mononuclear complexes.

Figs. 5c–e show the spectra of $CuCl_2{\cdot}2H_2O$ (5 mM) in MeOH with the addition of 1, 2 and 3 equiv of **1**, respectively. As **1** is added, different signals appear, indicating that **1** binds to the Cu^{2+} ion, to give a characteristic spectrum for the trinuclear Pt–Cu–Pt complex [20,36,39,40]. The spectrum in Fig. 5e shows a well-resolved profile with $g_{//} = 2.345$ and $g_{\perp} = 2.048$, which is characteristic of the unpaired electron residing in the Cu dx^2–y^2 orbital [20,36,39,40,45–49]. Both the $g_{//}$ and $g_{\perp}$ = signals are split into four components by the Cu nuclear hyperfine interaction ($A_{//} = 148 \times 10^{-4}\ cm^{-1}$ and $A_{\perp} = 18 \times 10^{-4}\ cm^{-1}$), accompanied with isotope effects arising from the natural occurrence of ^{63}Cu ($I = 3/2$, 69.1%) and ^{65}Cu ($I = 3/2$, 30.9%). In contrast, in the mixture of $CuCl_2{\cdot}2H_2O$ with 1 equiv of **1** (Fig. 5c), three sets of $g_{//}$ signals, all of which being split into four components, are observed, where the black and blue lines imply the original $CuCl_2{\cdot}2H_2O$ and trinuclear

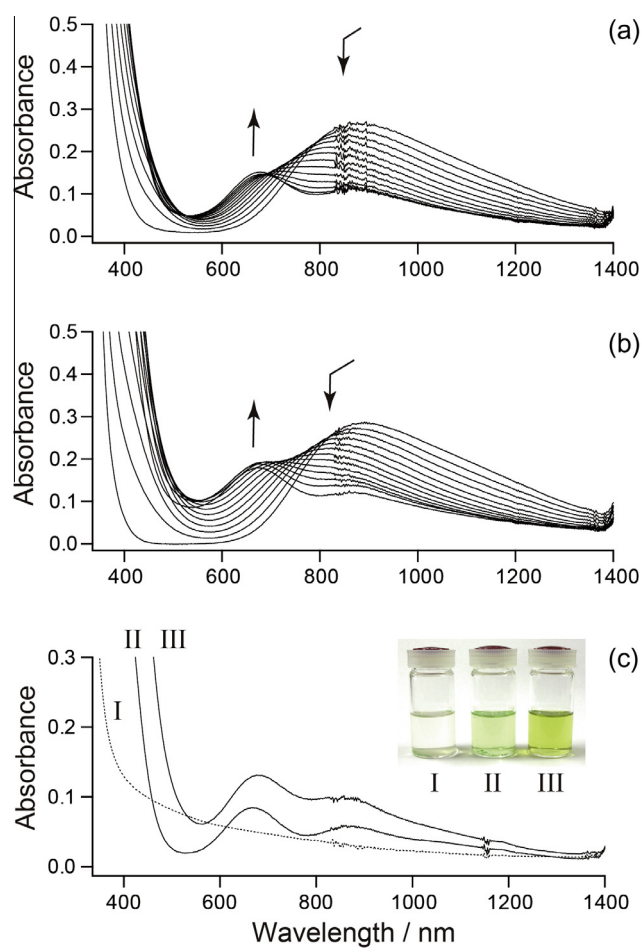

Fig. 6. UV–Vis spectra of a 5 mM solution of $CuCl_2{\cdot}2H_2O$ in MeOH containing 0–3 equiv. of (a) **2** and (b) **3** at room temperature. (c) The spectra of the supernatant after mixing $CuCl_2{\cdot}2H_2O$ (5 mM) and 2 equiv of **1**(I), **2**(II) or **3**(III) in $CHCl_3$, with a picture for each of the reaction mixtures.

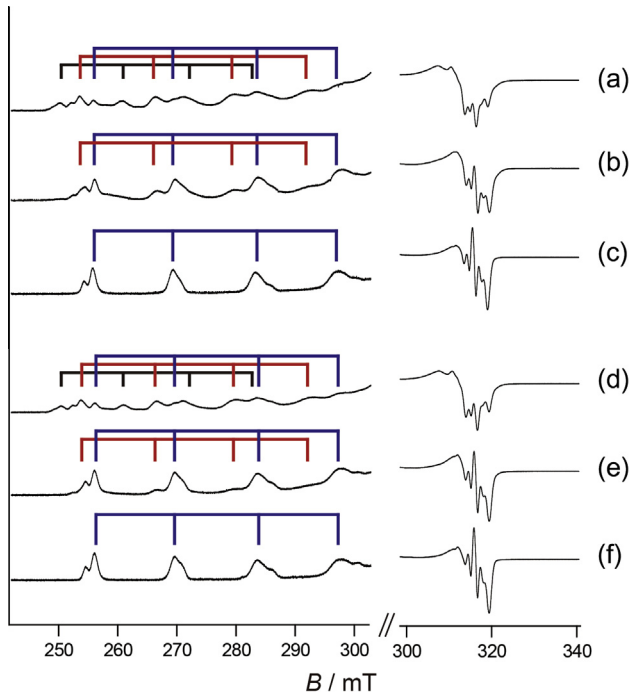

Fig. 7. Continuous wave EPR spectra in MeOH glass at 77 K for a mixture of $CuCl_2{\cdot}2H_2O$ (5 mM) and (a) **2** (5 mM), (b) **2** (10 mM), (c) **2** (15 mM), (d) **3** (5 mM), (e) **3** (10 mM) or (f) **3** (15 mM). Experimental settings: microwave frequency (a) 9.05255 GHz, (b) 9.06033 GHz, (c) 9.05113 GHz, (d) 9.05980 GHz, (e) 9.06025 GHz and (f) 9.05967 GHz; microwave power, 3 mW; field modulation, 0.2 mT.

Pt–Cu–Pt complexes, respectively, and the red line ($g_{//} = 2.365$, $A_{//} = 144 \times 10^{-4}\ cm^{-1}$) shows some different species. Taking into account the reaction processes, the species marked with red lines is the dinuclear Pt–Cu complex, as shown in Scheme 2, because both $g_{//}$ and $A_{//}$ values are intermediate between the values of the original $CuCl_2{\cdot}2H_2O$ and trinuclear Pt–Cu–Pt complex.

3.6. UV–Vis and EPR spectral titration of Cu^{2+} with **2** or **3**

Fig. 6a and b show the UV–Vis spectra of $CuCl_2{\cdot}2H_2O$ (5 mM) in MeOH with the addition of 0–3 equiv of **2** or **3**, where similar spectral changes were observed, indicating that both **2** and **3** also bind to Cu^{2+} ions. Although in the reaction with **1** the absorption band around 870 nm monotonically decreases in intensity, those in the reactions with **2** and **3** are slightly blue shifted with a decrease in intensity. In addition, the decreases in the absorption band heights around 870 nm were not terminated when 2 equiv of **2** or **3** had been added. Considering that the changes are caused by the formation of the crystallographically characterized 1:2 adduct, as mentioned above, the slight blue shifts and further decreases suggest that the trinuclear Pt–Cu–Pt complexes formed by **2** and **3** are less stable in MeOH than the complex formed by **1**.

Fig. 7a–c and d–f shows the EPR spectra in the titration of $CuCl_2{\cdot}2H_2O$ with **2** or **3**, respectively. Similarly to those with **1**, the spectral changes involve three kinds of species, $CuCl_2{\cdot}2H_2O$ (black lines), dinuclear Pt–Cu (red lines)[1] and trinuclear Pt–Cu–Pt (blue lines) complexes with similar *g* and *A* values to **1**. The remarkable difference is that the signal intensities for the dinuclear Pt–Cu complexes with Cu^{2+}:**2** = 1:1 (Fig. 7a) and Cu^{2+}:**3** = 1:1 (Fig. 7d) are larger than that with **1** (Fig. 5c), indicating that the ratio of dinuclear Pt–Cu complexes is larger. As well as the results of the UV–Vis spectra, the titrations with **2** and **3** do not terminate with a 1:2 ratio of Cu^{2+}:**2** or **3**, because the dinuclear Pt–Cu complexes still remain (Figs. 7b and e), whilst for **1** the dinuclear Pt–Cu complex has disappeared at Cu^{2+}:**1** = 1:2 (Fig. 5d). The larger populations of the dinuclear Pt–Cu complexes for **2** and **3** suggest that the alkyl chains, the propyl and butyl moieties, block the associations of the mononuclear Pt and dinuclear Pt–Cu complexes in MeOH.

Furthermore, there is an apparent difference in solubility between **1**, **2** and **3**. In spite of the ready solubility of **1** in H_2O, both **2** and **3** do not dissolve, but dissolve in $CHCl_3$ and CH_2Cl_2, which is attributed to the alkyl moieties. Fig. 6c shows the UV–Vis spectra for the supernatants of the $CHCl_3$ solution mixed with $CuCl_2{\cdot}2H_2O$ (5 mM) and 2 equiv of **1**, **2**, or **3**. As shown in the pictures in Fig. 6c, the supernatant containing $CuCl_2{\cdot}2H_2O$ and **1**(I) is transparent, whereas the mixtures with **2**(II) and **3**(III) are greenish. The spectra of II and III obviously show two characteristic bands attributed to the trinuclear Pt–Cu–Pt complexes, which were not observed in I. Considering that the absorption band intensity around 670 nm in III is larger than that in II, the concentration of the trinuclear Pt–Cu–Pt complex with **3** is larger. Actually, in the reaction vessel of **2**, some undissolved green crystals of $CuCl_2{\cdot}2H_2O$ remained. Therefore, the introduction of alkyl chains as co-ligands with the Pt atoms enhanced the hydrophobicity.

4. Conclusion

In summary, this work demonstrates the syntheses and characterization of two novel "amidate-hanging" Pt mononuclear complexes containing propyl and butyl amines. These alkyl amines enhance the hydrophobicity, showing the binding capability of Cu^{2+} ions in hydrophobic solvents, and the populations of intermediate dinuclear Pt–Cu complexes.

Acknowledgements

This work was supported by the Grants-in-Aid for Scientific Research (Scientific Research (C) 24550074) and Nippon Sheet Glass Foundation for Materials Science and Engineering.

Appendix A. Supplementary data

CCDC 949161-949163 contain the supplementary crystallographic data for **2**, **3** and **4**. These data can be obtained free of charge via http://www.ccdc.cam.ac.uk/conts/retrieving.html, or from the Cambridge Crystallographic Data Centre, 12 Union Road, Cambridge CB2 1EZ, UK; fax: +44 1223 336 033; or e-mail: deposit@ccdc.cam.ac.uk.

References

[1] C. Tejel, M.A. Ciriano, L.A. Oro, Chem. Eur. J. 5 (1999) 1131.
[2] K. Matsumoto, K. Sakai, Adv. Inorg. Chem. 49 (2000) 375.
[3] J.K. Bera, K.R. Dunbar, Angew. Chem. Int. Ed. 41 (2002) 4453.
[4] I.P.-C. Liu, W.-Z. Wang, S.-M. Peng, Chem. Commun. (2009) 4323.
[5] K. Mashima, Bull. Chem. Soc. Jpn. 83 (2010) 299.
[6] A. Erxleben, B. Lippert, J. Chem. Soc., Dalton Trans. (1996) 2329.
[7] W. Chen, F. Liu, K. Matsumoto, J. Autschbach, B.L. Guennic, T. Ziegler, M. Maliarik, J. Glaser, Inorg. Chem. 45 (2006) 4526.
[8] W. Chen, F. Liu, D. Xu, K. Matsumoto, S. Kishi, M. Kato, Inorg. Chem. 45 (2006) 5552.
[9] R. Hayoun, D.K. Zhong, A.L. Rheingold, L.H. Doerrer, Inorg. Chem. 45 (2006) 6120.
[10] I.P.-C. Liu, G.-H. Lee, S.-M. Peng, M. Bénard, M.-M. Rohmer, Inorg. Chem. 46 (2007) 9602.
[11] G. Givaja, O. Castillo, E. Mateo, A. Gallego, C.J. Gómez-García, A. Calzolari, Chem. Eur. J. 18 (2012) 15476.
[12] E.W. Dahl, F.G. Baddour, S.R. Fiedler, W.A. Hoffert, M.P. Shores, G.T. Yee, J.-P. Djukic, J.W. Bacon, A.L. Rheingold, L.H. Doerrer, Chem. Sci. 3 (2012) 602.
[13] F.G. Baddour, S.R. Fiedler, M.P. Shores, J.A. Golen, A.L. Rheingold, L.H. Doerrer, Inorg. Chem. 52 (2013) 4926.

[1] For interpretation of color in Fig. 7, the reader is referred to the web version of this article.

[14] K. Uemura, K. Fukui, H. Nishikawa, S. Arai, K. Matsumoto, H. Oshio, Angew. Chem. Int. Ed. 44 (2005) 5459.
[15] K. Uemura, K. Fukui, K. Yamasaki, K. Matsumoto, Sci. Technol. Adv. Mater. 7 (2006) 461.
[16] K. Uemura, K. Yamasaki, K. Fukui, K. Matsumoto, Eur. J. Inorg. Chem. (2007) 809.
[17] K. Uemura, K. Fukui, K. Yamasaki, K. Matsumoto, M. Ebihara, Inorg. Chem. 49 (2010) 7323.
[18] K. Uemura, M. Ebihara, Inorg. Chem. 50 (2011) 7919.
[19] K. Uemura, K. Sakurai, E. Yasuda, M. Ebihara, Polyhedron 45 (2012) 35.
[20] K. Uemura, M. Ebihara, Inorg. Chem. 52 (2013) 5535.
[21] W. Chen, F. Liu, T. Nishioka, K. Matsumoto, Eur. J. Inorg. Chem. (2003) 4234.
[22] W. Chen, K. Matsumoto, Inorg. Chim. Acta. 342 (2003) 88.
[23] L. Maresca, G. Natile, F.P. Intini, F. Gasparrini, A. Tiripicchio, M. Tiripicchio-Camellini, J. Am. Chem. Soc. 108 (1986) 1180.
[24] R. Cini, F.P. Fanizzi, F.P. Intini, L. Maresca, G. Natile, J. Am. Chem. Soc. 115 (1993) 5123.
[25] A. Erxleben, I. Mutikainen, B. Lippert, J. Chem, J. Chem. Soc., Dalton Trans. (1994) 3667.
[26] R. Cini, P.A. Caputo, F.P. Intini, G. Natile, Inorg. Chem. 34 (1995) 1130.
[27] R. Cini, F.P. Fanizzi, F.P. Intini, C. Pacifico, G. Natile, Inorg. Chim. Acta. 264 (1997) 279.
[28] R. Cini, A. Cavaglioni, F.P. Intini, F.P. Fanizzi, C. Pacifico, G. Natile, Polyhedron 18 (1999) 1836.
[29] K. Uemura, K. Yamasaki, K. Fukui, K. Matsumoto, Inorg. Chim. Acta. 360 (2007) 2623.
[30] S.C. Dhara, Indian J. Chem. (1970) 193.
[31] F.D. Rochon, V. Buculei, Inorg. Chim. Acta. 357 (2004) 2218.
[32] Rigaku, REQAB. Version 1.1., Rigaku Corporation, Tokyo, Japan, 1998.
[33] A. Altomare, M.C. Burla, M. Camalli, G.L. Cascarano, C. Giacovazzo, A. Guagliardi, A.G.G. Moliterni, G. Polidori, R. Spagna, J. Appl. Crystallogr. 32 (1999) 115.
[34] G.M. Sheldrick, Acta Crystallogr. A64 (2008) 112.
[35] K. Wakita, Yadokari-XG, Software for crystal structure analyses (2001), in: C. Kabuto, S. Akine, T. Nemoto, E. Kwon (Eds.), Release of Software (Yadokari-XG 2009) for Crystal Structure Analyses, J. Cryst. Soc. Jpn. 51(3) (2009) 218–224.
[36] B. Lippert, U. Thewalt, H. Schöllhorn, D.M.L. Goodgame, R.W. Rollins, Inorg. Chem. 23 (1984) 2807.
[37] I. Mutikainen, O. Orama, A. Pajunen, Inorg. Chim. Acta. 137 (1987) 189.
[38] G. Frommer, F. Lianza, A. Albinati, B. Lippert, Inorg. Chem. 31 (1992) 2434.
[39] A. Schreiber, O. Krizanovic, E.C. Fusch, B. Lippert, F. Lianza, A. Albinati, S. Hill, D.M.L. Goodgame, H. Stratemeier, M.A. Hitchman, Inorg. Chem. 33 (1994) 6101.
[40] A. Erxleben, A. Albinati, B. Lippert, J. Chem. Soc., Dalton Trans. (1996) 1823.
[41] W. Chen, K. Matsumoto, Eur. J. Inorg. Chem. (2002) 2664.
[42] C. Chen, H. Qiu, F. Liu, W. Chen, J. Chem. Crystallogr. 37 (2007) 619.
[43] M.-E. Moret, P. Chen, Eur. J. Inorg. Chem. (2010) 438.
[44] D.M.L. Goodgame, M.A. Hitchman, B. Lippert, Inorg. Chem. 25 (1986) 2191.
[45] H. Yokoi, T. Isobe, Bull. Chem. Soc. Jpn. 39 (1966) 2054.
[46] S. Antosik, N.M.D. Brown, A.A. McConnell, A.L. Porte, J. Chem, A (1969) 545.
[47] I. Adato, I. Eliezer, J. Chem. Phys. 54 (1971) 1472.
[48] H. Yokoi, T. Kishi, Chem. Lett. (1973) 749.
[49] D. Collison, D.M.L. Goodgame, M.A. Hitchman, B. Lippert, F.E. Mabbs, E.J.L. McInnes, Inorg. Chem. 41 (2002) 2826.